Astron. Astrophys. 358, 605–611 (2000)

ASTRONOMY AND ASTROPHYSICS

A deep search for the optical counterpart to the anomalous X-ray pulsar 1E 2259+58.6

F. Hulleman[1], **M.H. van Kerkwijk**[1], **F.W.M. Verbunt**[1], **and S.R. Kulkarni**[2]

[1] Astronomical Institute, Utrecht University, P.O. Box 80000, 3508 TA Utrecht, The Netherlands
[2] Palomar Observatory, California Institute of Technology 105-24, Pasadena, CA 91125, USA

Received 10 January 2000 / Accepted 9 March 2000

Abstract. We present Keck R and I band images of the field of the anomalous X-ray pulsar 1E 2259+58.6. We derive an improved X-ray position from archival ROSAT HRI observations by correcting for systematic (boresight) errors. Within the corresponding error circle, no object is found on the Keck images, down to limiting magnitudes $R = 25.7$ and $I = 24.3$. We discuss the constraints imposed by these limits, and conclude that it is unlikely that 1E 2259+58.6 is powered by accretion from a disk, irrespective of whether it is in a binary or not, unless the binary is extremely compact.

Key words: stars: pulsars: individual: 1E 2259+58.6 – accretion, accretion disks – stars: neutron – stars: white dwarfs – X-rays: stars

1. Introduction

There is a growing number of X-ray pulsars for which it is not clear why they emit X-rays. Their rotational energy loss appears insufficient to power the X-ray luminosity and there is no sign of a companion from which they could accrete matter. These pulsars are called the "anomalous X-ray pulsars" (AXP).

The AXP differ from other X-ray pulsars in the following properties (Hellier 1994, Mereghetti & Stella 1995, van Paradijs et al. 1995): (i) their spin periods are within a small range, between 5 and 9 seconds, and their spin-down rates are nearly constant; (ii) timing analysis gives no evidence of orbital motion; (iii) their X-ray spectra are rather soft; (iv) their X-ray light curves show less variability; (v) their inferred X-ray luminosities are rather low ($\sim 10^{35}\,\mathrm{erg\,s^{-1}}$); (vi) they are located close to the Galactic plane; (vii) some appear associated with supernova remnants.

Members of the group of AXP include 4U 0142+61, 1E 2259+58.6, 1E 1048.1−5937 and RX J1838.4−0301 (Mereghetti & Stella 1995 and references therein). Recently, three X-ray pulsars with similar properties were discovered: 1RXS J170849.0−400910 (Sugizaki et al. 1997); 1E 1841−045 in the supernova remnant Kes 73 (Vasisht & Gotthelf 1997); and AX J1845.0−0300 (Torii et al. 1998; Gotthelf & Vasisht 1998) in the supernova remnant G29.6+0.1 (Gaensler et al. 1999). Indeed, perhaps even the progeny of these systems has been identified, in RX J0720.4−3125 (Haberl et al. 1997). The latter object is the only one for which the optical counterpart has been identified (Motch & Haberl1998; Kulkarni & van Kerkwijk 1998).

A variety of models for AXPs has been put forward, using both accretion and intrinsic mechanisms to explain the X-ray luminosity. For the accretion scenarios, the source of matter has been suggested to be a very low mass companion (Mereghetti & Stella 1995) or a circumstellar disk composed of debris, either from a common envelope phase of a high mass X-ray binary (van Paradijs et al. 1995; Ghosh et al. 1997) or from a supernova explosion (Corbet et al. 1995; Chatterjee et al. 1999). In scenarios in which the X-ray emission is intrinsic, the sources are either hot, massive, rapidly spinning white dwarfs, formed in the merger of a double white-dwarf binary (Paczyński 1990), or so-called "magnetars," isolated neutron stars with very high magnetic field strengths ($\gtrsim 10^{14}\,\mathrm{G}$; Thompson & Duncan 1996). In the latter case, AXP might be related to soft gamma-ray repeaters[1].

In this paper, we present a deep search for the optical counterpart to the AXP 1E 2259+58.6. In Sect. 2, we briefly review what is known about this source. We derive a refined position for 1E 2259+58.6 in Sect. 3, and in Sect. 4 we present our optical observations. We discuss the results in Sect. 5.

2. 1E 2259+58.6

1E 2259+58.6 is located inside the supernova remnant CTB 109 (G109.1−1.0). This remnant is semi-circular, with neither X-ray nor radio emission from its western side (see, e.g., Rho & Petre 1997), which may be related to the presence of a molecular cloud. A lobe of enhanced X-ray emission ('jetlike' feature) is present in between the eastern shell and the pulsar, but likely this does not reflect physical interaction.

1E 2259+58.6 is an X-ray pulsar with a period of 6.98 s. It is observed to be spinning down with a period derivative of

Send offprint requests to: F.Hulleman@astro.uu.nl

[1] The proposed X-ray counterparts to SGRs also have spin periods in the 5–9 s range (Kouveliotou et al. 1998, 1999).

$5.5 \times 10^{-13}\,\mathrm{s\,s^{-1}}$. Baykal & Swank (1996) found small but significant deviations from constant spin-down and concluded that accretion must be the source of energy (but see Melatos 1999 for a different explanation). An upper limit $a_{\rm X} \sin i < 0.03$ lt-s has recently been obtained with the RXTE (Mereghetti et al. 1998). Assuming a Roche-lobe filling companion and an orbital inclination $i > 30°$, this restricts the companion mass to $\lesssim 0.1 M_\odot$ for a main-sequence star, and to $\lesssim 0.8 M_\odot$ for a helium-burning star. No constraint can be set for a white-dwarf companion.

1E 2259+58.6 has a very soft X-ray spectrum, best described by a combination of a power-law with photon index 4.0 ± 0.1 and a blackbody with $kT = 0.43 \pm 0.02\,\mathrm{keV}$, absorbed by a column density $N_{\rm H} = 8.5 \pm 0.4 \times 10^{21}\,\mathrm{cm^{-2}}$ (Rho & Petre 1997 using ASCA, BBXRT and ROSAT PSPC data; see also Corbet et al. 1995). A possible problem is contamination of the spectrum by extended emission around the pulsar (Rho & Petre 1997). Parmar et al. (1998) tried to account for this by subtracting the observed spectrum of the supernova remnant multiplied with a scale factor. They find that the residual spectrum can be fitted with a simple power law with an absorption column density of $N_{\rm H} = (2.18 \pm 0.07) \times 10^{22}\,\mathrm{cm^{-2}}$. It should be noted, however, that the BeppoSAX LECS and MECS instruments used by these authors have rather poor spatial resolution. Furthermore, Rho & Petre (1997) found that the spectral shape of the extended emission near 1E 2259+58.6 differs from that of the remnant.

No radio counterpart to 1E 2259+58.6 has been found down to an upper limit of $50\,\mu$Jy (Coe et al. 1994). So far, no counterpart at optical and infrared wavelengths could be identified (Davies & Coe 1991; Coe & Pightling 1998). These authors obtained limiting magnitudes of B = 25, V = 24, R = 24.5, I = 23, H = 18.5, J = 19.6 and K = 18.4, although they could not exclude several candidates due to the fact that the X-ray position of 1E 2259+58.6 was not known accurately enough. Note that their astrometry differs from ours and that of Fahlman et al. (1982) (see Sect. 3 and Davies & Coe 1991).

2.1. Distance and reddening to 1E 2259+58.6

All distance estimates to 1E 2259+58.6 use distances to either CTB 109 or the molecular cloud, i.e., it is assumed that the pulsar is at the same distance as CTB 109 and that the molecular cloud is either at the same distance as well or in front (and causes the absence of emission from the western part of the CTB 109). The distance to CTB 109 was estimated using the surface brightness diameter relation by Sofue et al. (1983) and Hughes et al. (1984), at 4.1 and 5.6 kpc, respectively. A lower limit to the distance of $d \gtrsim 6 \pm 1\,\mathrm{kpc}$ was obtained by Strom (priv.comm) from hydrogen 21-cm line absorption measurements towards the remnant (Braun & Strom 1986).

For the molecular cloud, a kinematic distance of $5 \pm 1\,\mathrm{kpc}$ can be derived from the molecular line measurements of Kahane et al. (1985) (here, we used the linear fit to the galactic rotation curve of Fich et al. 1989, with rotation constants $\Theta_0 = 220\,\mathrm{km\,s^{-1}}$ and $R_0 = 8.5\,\mathrm{kpc}$). Distance estimates have also been made for several H II regions associated with the molecular cloud. Spectrophotometric parallaxes for the exciting stars were obtained by Crampton et al. (1978), leading to distances of 5.5, 5.6, 3.6 and 4.0 kpc for the H II regions S148, S149, S152 and S153, respectively. Furthermore, a lower limit of $d \gtrsim 6 \pm 1\,\mathrm{kpc}$ towards S152 was obtained by Strom (priv.comm) using hydrogen 21-cm line absorption. From the above, assuming that the fractional errors in the spectrophotometric parallaxes are about 25% (corresponding to uncertainties of about 0.5 mag in the absolute magnitudes inferred from the spectral types), we conclude that a distance to the molecular cloud of $5 \pm 1\,\mathrm{kpc}$ is most likely, and, therefore, that 1E 2259+58.6 is at $d \gtrsim 5 \pm 1\,\mathrm{kpc}$.

The reddening to 1E 2259+58.6 can be estimated from the X-ray hydrogen column density using the relation $N_{\rm H} = (1.79 \pm 0.03) \times 10^{21}\,A_V\,\mathrm{cm^{-2}}$, where A_V is the visual extinction in magnitudes (Predehl & Schmitt 1995). From the fits to the X-ray spectrum of Rho & Petre (1997), values of $N_{\rm H}$ between 0.8 and $1.2 \times 10^{22}\,\mathrm{cm^{-2}}$ are found, with a best fit value of $0.85 \times 10^{22}\,\mathrm{cm^{-2}}$. Thus, one infers $A_V = 4.5$ to 6.7 mag, with a best-fit value of 4.7 mag. For $N_{\rm H} = 2.18 \times 10^{22}\,\mathrm{cm^{-2}}$, as found by Parmar et al. (1998), one would infer $A_V = 12.2$ mag. As noted above, however, we feel this measurement is rather uncertain.

The reddening can be estimated indirectly using CTB 109. Fesen & Hurford (1995) measured Hα and Hβ relative line intensities in optical spectra of 5 filaments, and found $A_V = 2.5$ to 3.7 mag, with substantial variations across the remnant. These values appear somewhat lower than those derived above from the X-ray absorption for 1E 2259+58.6, and thus one may wonder about the association, or about possible intrinsic absorption around 1E 2259+58.6. Since the reddening to the remnant is seen to vary, however, a somewhat higher value for 1E 2259+58.6 does not seem unlikely. Furthermore, from the X-ray emission of CTB 109, column densities corresponding more closely to that of 1E 2259+58.6 are inferred (Rho & Petre 1997).

In the following, we will adopt a reddening of $A_V = 4.7$ mag and a distance of 6 kpc, unless noted otherwise.

3. Improved X-ray position

1E 2259+58.6 has been in the field of view of two observations with the ROSAT high resolution imager (HRI; David et al. 1999). The first was in 1992 from January 8, 07:16 UT, to January 10, 18:59 UT, and was centered on 1E 2259+58.6. The second was pointed at the lobe to the East of the pulsar and was from June 25, 07:46 UT, to June 27, 08:26 UT. In both observations, the semicircular shell, the lobe, the pulsar and the extended emission in its immediate surroundings, as well as three other point sources can be seen. We identify the latter with sources 1, 2 and 3 in Table 4 of Rho & Petre (1997), and will refer to these as RP1, RP2 and RP3 hereafter.

The data were analysed using the EXSAS software package (1998 April version) in the following way. First, we corrected for the small error in HRI plate scale found by Hasinger et al. (1998), by multiplying all detector positions (relative to the detector centre) with a factor 0.9972. Next, we ran the standard source

Table 1. X-ray and optical positions used for the astrometry.

Source	$\alpha_{\rm J2000}$	$\delta_{\rm J2000}$	$\sigma_{\alpha,\delta}$ [a]
RP1 – HRI			
January 1992	23 00 32.85	58 52 51.9	0.9
June 1992	23 00 33.98	58 52 49.5	2.3
RP1 – counterpart			
1425-14436845[b]	23 00 33.396	58 52 47.16	0.2
DSS1 1953.830	23 00 33.393	58 52 47.22	0.2
DSS2 1991.671	23 00 33.377	58 52 47.07	0.2
RP3 – HRI			
January 1992	23 03 19.41	58 45 33.9	1.3
June 1992	23 03 20.30	58 45 26.4	1.5
RP3 – counterpart			
1425-14515707[b]	23 03 19.472	58 45 28.95	0.2
DSS1 1953.830	23 03 19.471	58 45 28.43	0.2
DSS2 1991.671	23 03 19.578	58 45 28.68	0.2
1E 2259+58.6 – HRI			
January 1992	23 01 08.09	58 52 48.3	0.1
June 1992	23 01 08.99	58 52 45.3	0.1
1E 2259+58.6– corrected			
Using RP1 and RP3	23 01 08.44	58 52 44.1	0.9
Using RP1 only	23 01 08.62	58 52 43.5	1.3

[a] Uncertainty in each coordinate (in arcsec).
[b] USNO-A2 identifier; mean epoch 1953.830.

detection program, which creates a preliminary source list using a sliding cell algorithm. This source list is fed into a maximum likelyhood detection algorithm (Cruddace et al. 1988), which yields precise positions (see Zimmermann et al. 1998). In order to prevent trouble with the extended emission from the remnant, we used two masks, one to the East of CTB 109 containing RP3 and one to the West containing RP1, RP2 and 1E 2259+58.6. Our final positions are listed in Table 1; the 1-σ errors are internal, i.e., they do not yet include pointing uncertainties. We verified that different choices of mask images gave consistent results.

Comparing the positions derived for the two observations (Table 1), it is clear that they are not consistent. This reflects the uncertainties in the attitude solutions used to transform detector positions to sky positions (see, e.g., David et al. 1999). One can correct for this if one has independent positions for some of the sources, for instance from optical counterparts. Below, we will try to do this.

Many X-ray sources can be identified with bright stars; for instance, Motch et al. (1998) find that 85% of the sources in a galactic plane region are bright stars. Therefore, we searched the USNO-A2.0 catalogue (Monet et al. 1998) for bright stars ($r_{\rm usnoa2} < 13.0$) near the positions of RP1, RP2 and RP3. We tentatively identify RP1 and RP3 with stars USNO-A2 1425-14436845 and USNO-A2 1425-14515707, respectively. No bright star was found within $30''$ of the position of RP2. We derived proper motions for the two stars by measuring positions on first and second generation images from the digitized sky survey, using astrometry relative to the USNO-A2.0 catalogue[2] (Table 1). For USNO-A2 1425-14515707, we found a significant proper motion of $0\farcs022 \pm 0\farcs004\,{\rm yr}^{-1}$ at position angle $90\fdg7 \pm 10\fdg2$.

The refined position for 1E 2259+58.6 was derived as follows. First, the HRI positions were shifted to a common reference using the positions of 1E 2259+58.6. Next, we determined weighted average offsets in right ascension and declination between the HRI and optical positions (including proper motion). For this purpose, we weigh the four individual offsets in right ascension and declination (RP1 and RP3; two HRI observations) using the uncertainties given by the source detection algorithm (the errors in the optical positions are much smaller, $\sim 0\farcs2$).

The differences with the weighted average correspond to $\chi^2 = 11.5$ for 6 degrees of freedom. This is not a good fit and suggests the presence of additional systematic errors. Following Hasinger et al. (1998), we added an error $E_{\rm sys}$ in quadrature to the individual measurement errors such that $\chi^2_{\rm red} \simeq 1$. For this purpose, we require $E_{\rm sys} = 1\farcs0$. Including this additional uncertainty, we infer that our corrected position of 1E 2259+58.6, listed in Table 1, has an uncertainty of $0\farcs9$ in each coordinate. This corresponds to a 95% confidence error radius of $2\farcs2$.

The value of $E_{\rm sys}$ we find is twice the value used by Hasinger et al. (1998). While these authors also included an $0\farcs5$ uncertainty in optical positions, we wondered whether the somewhat large required value might be related to the rather large offset from the center of RP3. To get a feeling for the uncertainty, we also determined a corrected position using RP1 only. The position is shifted slightly and has a slightly larger uncertainty of $1\farcs3$ in each coordinate (see Table 1). The 95% confidence error circle for this case has a radius of $3\farcs3$.

We show both error circles superposed on Keck images in Fig. 1. Also indicated are the positions determined previously by Fahlman et al. (1982; short dashed) and Hanson et al. (1988; long dashed). Note that all these positions differ significantly from that of Coe & Pighting (1998). We do not understand the reason for this discrepancy.

4. Keck observations

Optical (R and I band) images of the field around 1E 2259+58.6 were obtained on 1994 October 30/31 and 1997 January 7 using the Low-Resolution Imaging Spectrometer (LRIS, Oke et al. 1995) at the Cassegrain focus of the Keck I (1994) and Keck II (1997) telescopes. The 1994 observations were plagued by clouds and high cirrus; the seeing was $1\farcs1$. All 1994 images have a large gradient in the sky background. As a result, all but one of these images are useless. In 1997, the weather was photometric, but the seeing mediocre at $1\farcs2$. All images were bias subtracted and flat fielded using dome flats. Unfortunately, it turned out that in the 1997 R-band images the position of 1E 2259+58.6 was very close to a region of lower sensitivity in the CCD, which did not flat-field out. The resulting "smear" is

[2] Note that both DSS1 and USNO-A2.0 positions were derived from the same plate and the results should therefore agree. The slight discrepancy in declination for RP3 is probably due to a second (fainter) star close to the proposed counterpart. This does however not affect our results.

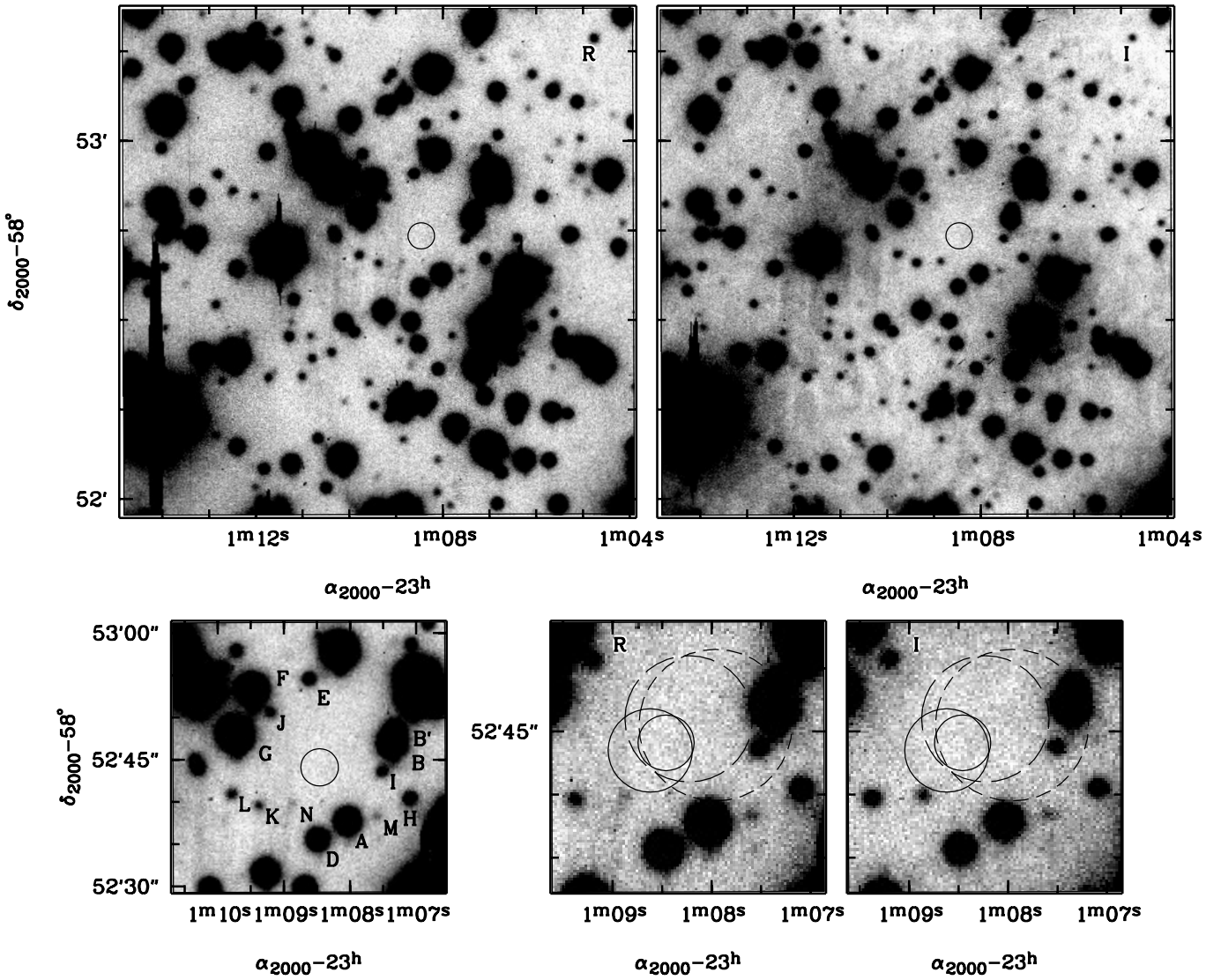

Fig. 1. R and I band images around 1E 2259+58.6, the circle is the 95% confidence circle obtained in Sect. 3. This circle is also shown in the lower three enlarged images, where one has the star identifications and two have the conservative Rosat error circle at 95% confidence and previous error circles obtained by Fahlman et al. (1982; short dashed) and Hanson et al. (1988; long dashed) superposed.

just over stars K and N in two of the three images; it can also be seen in Fig. 1).

Astrometry was done using a short (300 s) R band image from 1997. We identified objects with stars in the USNO-A2.0 catalogue and obtain centroids for objects that were not saturated and appeared stellar (i.e., had a sufficiently small diameter). Next, we applied a bi-cubic distortion correction (J. Cohen, 1997, private comm.), and solved for zero-point position, scale, and position angle by comparison with the USNO-A2.0 positions. After rejecting six outliers (probably misidentifications or large proper motion objects), the remaining 134 objects gave a good solution. The root-mean-square displacement from the catalogued positions is 0.26″ in right ascension and 0.25″ in declination.

For the photometry, we used the DAOPHOT II software package (Stetson 1987). Instrumental magnitudes were obtained from two R band images (one from 1994 and one from 1997, 1000s exposure each) and the average of two I band images (300s each, 1997 only). We calibrated the photometry using the magnitudes determined by Davies & Coe (1991). The apparent magnitudes of selected objects as determined from the 1997 observations are listed in Table 2. The values derived for the 1994 R-band image are consistent with these, but have lower accuracy. Note that the uncertainties listed in the table are the formal 1σ fitting errors. In addition to these, there are systematic uncertainties related to the zero point. Since Davies & Coe (1991) found a discrepancy by about 0.15 mag in magnitudes obtained from two different exposures, the zero-point uncertainty is probably of the order of 0.1 mag.

No object is found inside either of the HRI error circles derived above. We derived lower limits with the help of simulations. For these, we took the mean of the three 1997 R band

Table 2. Apparent magnitudes[a] of selected stars in the field around 1E 2259+58.6. Star designations are after Davies & Coe (1991).

Star	R	I	$R-I$
A	19.697 ± 0.003	18.577 ± 0.005	1.120 ± 0.006
B	19.265 ± 0.003	18.217 ± 0.005	1.048 ± 0.006
B'	21.206 ± 0.010	19.987 ± 0.011	1.219 ± 0.015
D	20.409 ± 0.004	19.274 ± 0.005	1.135 ± 0.006
E	22.537 ± 0.016	22.545 ± 0.043	-0.008 ± 0.046
F	18.902 ± 0.004	17.904 ± 0.007	0.998 ± 0.008
H	22.398 ± 0.014	21.219 ± 0.014	1.179 ± 0.020
I	23.024 ± 0.023	21.672 ± 0.020	1.352 ± 0.030
J	23.131 ± 0.027	21.473 ± 0.019	1.658 ± 0.033
K	23.676 ± 0.037	21.297 ± 0.015	2.379 ± 0.040
L	23.389 ± 0.028	21.799 ± 0.028	1.590 ± 0.040
M	24.557 ± 0.086	22.832 ± 0.068	1.745 ± 0.110
N	24.848 ± 0.110	22.119 ± 0.031	2.729 ± 0.114

[a] In addition to the listed uncertainties, there is a 0.1 mag uncertainty in the zero point; see text.

images and selected the inner region of the image that is void of stars. Next, we placed an artificial star with magnitude M at a random spot in this region and determined its magnitude in the same way as for the real objects (this also allowed us to verify the errors quoted in the table). This was done ten times for a number of values of M, within a range 25.0–26.9 for R and 23.7–25.7 mag for I. We define the 3σ detection threshold to be that magnitude M for which the standard deviation equals 0.3 mag. Taking account of the fact that we need about 3 trials to cover the error circle, the derived 2σ limits are $R > 25.7$ and $I > 24.3$ (for the error circle derived using RP1 only we need 7.5 trials and obtain $R > 25.6$ and $I > 24.2$).

5. Discussion

We now examine the limits on the optical emission imposed by the various models proposed for 1E 2259+58.6. Contributions to the optical flux can come from the object itself, an accretion disk and a companion star. We will discuss these, in the context of the proposed models, in the following subsections.

5.1. An isolated object

Paczyński (1990) proposed that 1E 2259+58.6 is a rapidly rotating, hot, massive, hot white dwarf, formed in the merger of two normal white dwarfs. Such a rapidly rotating white dwarf can have sufficient rotational energy loss ($\sim 10^{36}\,\mathrm{erg\,s^{-1}}$) to power the observed X-ray flux. Using blackbody emission and a white dwarf radius of $0.002\,R_\odot$, our optical limits correspond to a maximum temperature $kT = 0.4\,\mathrm{keV}$. Since the Eddington condition gives a maximum temperature of $kT = 0.2\,\mathrm{keV}$ (Paczyński 1990), our data can thus not exclude this model.

Similarly, our limits do not allow us to constrain the magnetar model. (A very crude estimate gives $R \simeq 36$ for a $kT = 0.4\,\mathrm{keV}$ blackbody at $d = 6\,\mathrm{kpc}$ and reddened by $A_R = 3.8$.)

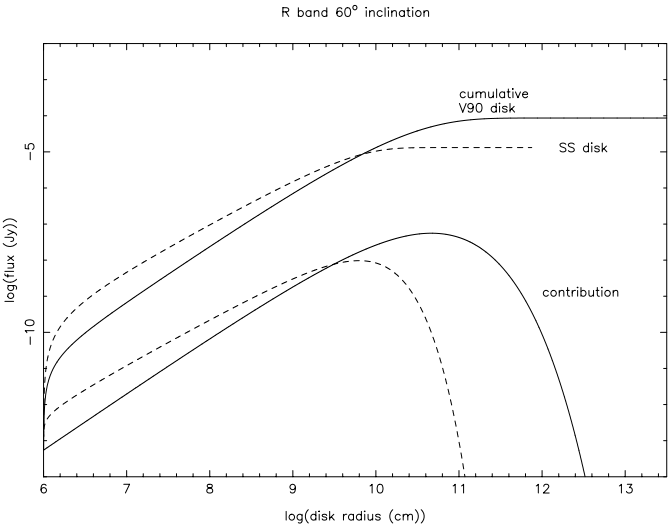

Fig. 2. Cumulative R band flux observed at earth as a function of radius for irradiated (solid line) and unirradiated (dashed line) disks at a distance of 6 kpc. The lower curves show the contribution of the flux for individual disk annuli (at constant $\Delta \log r$). No correction was made for reddening.

5.2. An isolated NS accreting from a disk

We will make an estimate for the optical emission of an accretion disk using two simple models. In the first, we use the $T(r) \propto r^{-3/7}$ relation expected for an accretion disk dominated by irradiation (labeled V90 hereafter; Vrtilek et al. 1990). An important assumption in obtaining this relation is that the disk is isothermal in the vertical direction, due to the irradiation. The second model we use is a Shakura-Sunyaev disk (labeled SS; Shakura & Sunyaev 1973), in which the energy generated by the disk itself is taken into account but irradiation is neglected. For both models, we assume the disk emits like a blackbody. We believe the first model should be the more reasonable approximation (at least for radii larger than a few 10^{10} cm; for smaller radii, this model underestimates the emission; see Fig. 2), while the second model should give a conservative limit.

Fig. 2 shows predicted R-band fluxes as a function of disk radius for a disk inclined by 60° relative to the line of sight, located at a distance of 6 kpc, and either irradiated by a central X-ray source with $L_\mathrm{X} = 4.3 \times 10^{35}\,\mathrm{erg\,s^{-1}}$ (V90), or not irradiated (SS). Also shown is the contribution to the total flux from each radius r (at constant $\Delta \log r$). There is no significant contribution to the flux for radii larger than $\sim 10^{12}$ cm (V90) and $\sim 10^{11}$ cm (SS), because the temperature becomes too low. For a large disk around an isolated neutron star, we find $R = 22.7$ for the V90 disk ($r \geq 10^{12}$ cm; $i = 60°$), and $R = 24.7$ for the SS disk ($r \geq 10^{11}$ cm; $i = 60°$). Here, for both estimates we used an R-band extinction $A_R = 3.8$, which corresponds to $A_V = 4.7$ (see Sect. 2.1).

From the above limits, we conclude that it is unlikely that 1E 2259+58.6 is an isolated NS accreting from a disk. Only if we underestimated the reddening considerably or if the disk inclination were very unfavourable, a (large) accretion disk could

have escaped detection. Increasing the distance to the source is not an option, since the optical emission of the disk is proportional to the X-ray emission. (for the SS disk model at 10 kpc, we still expect $R = 25.1$).

5.3. A very low mass binary

The optical emission of low mass X-ray binaries is dominated by the emission from the accretion disk surrounding the compact object. An empirical relationship, $M_{\rm V} = (1.57 \pm 0.24) - (2.27 \pm 0.32) \times \log[(L_{\rm X}/L_{\rm edd})^{1/2}(P/1\,{\rm hr})^{2/3}]$, was found by van Paradijs & McClintock (1994). Assuming $(V-R)_0 \sim 0$, according to this relationship a putative binary must have $P \lesssim 10^2$ s in order to remain below our detection limit $R > 25.7$. This would rule out all but a white dwarf counterpart. There is considerable scatter around the relation, however, and period estimates will be off by a factor of 5 for a change of 1 mag. Furthermore, it is far from clear one can extrapolate their result to such short periods.

Given the above, it is perhaps more relevant to compare our limits with the emission from the compact low-mass X-ray binary 4U 1626−67 (Chakrabarty 1998). Indeed, this source has a number of the properties of AXP (Mereghetti & Stella 1995; cf. van Paradijs et al. 1995). Under the assumption that 4U 1626−67 and 1E 2259+58.6 have the same $L_{\rm X}/L_{\rm opt}$ ratio, the expected magnitude would be $R = 24.8$. Here, we have taken account of the difference in X-ray flux of about a factor ten (compare, e.g., Orlandini et al. 1998 and Parmar et al. 1998), as well as the difference in reddening towards the two sources. Even if the X-ray flux of 1E 2259+58.6 were only one twentieth that of 4U 1626−67, we would still expect to have detected the optical counterpart at $R = 25.5$. Thus, we conclude that most likely even such a compact binary would have been detected.

What would our limits imply if there were no accretion disk present and the optical emission was dominated by the companion star? This seems unlikely, but might perhaps be the case if accretion is from a (irradiation-induced) stellar wind. We will discuss two possible companions below: (i) a main-sequence star; (ii) a He-burning star. From Sect. 5.1) above, it will be clear that we can put no meaningful constraints for the case the only source of optical emission is a white-dwarf companion.

Based on the colors derived from model spectra by Bessell et al. (1998) (overshoot models, their Table 1, for $\log g = 4.5$), we find that a main-sequence companion to 1E 2259+58.6 would have to be of type K or later to escape detection.

To start helium burning, a star's mass must exceed $\sim 0.3 M_\odot$. From Savonije et al. (1986), we find that a $\sim 0.3 M_\odot$ helium burning star has $T_{\rm eff} \simeq 20000$ K and $L \simeq 0.6 L_\odot$. Using Table 3 of Bessell et al. (1998), we infer a bolometric correction of -2.0 and $V - R = -0.1$ for a 20000 K star (note that this table does not extend to $\log g > 5$, but since the variation with $\log g$ is small, our extrapolation should be safe). For these values, the star would have $R = 25.1$ and $I = 24.1$, which is just above our detection limit. More massive stars would be brighter, and, thus, the companion cannot be a star burning helium.

6. Conclusions

We have shown that the tight limits we derive on the optical emission of 1E 2259+58.6 are a serious problem for scenarios involving accretion by way of an accretion disk. This is irrespective of whether the source is in a binary, except if the binary is extremely compact. Therefore, we conclude that, most likely, 1E 2259+58.6 is an isolated object, and that its emission is not powered by accretion. We note that the same conclusion was indepently drawn by Kaspi et al. (1999) on the basis of the extreme rotational stability of 1E 2259+58.6.

Acknowledgements. We would like to thank Richard Strom for discussions about the distance to 1E 2259+58.6. We have made use of the ROSAT Data Archive of the Max-Planck-Institut für Extraterrestrische Physik (MPE) at Garching, Germany, of the SIMBAD database operated at CDS, Strasbourg, France, and of the Digitized Sky Surveys, which were produced at the Space Telescope Science Institute from photographic data obtained using the Oschin Schmidt Telescope on Palomar Mountain. We acknowledge support of a fellowship of the Royal Netherlands Academy of Arts and Sciences (MHvK) and grants from NASA and NSF (SRK).

References

Baykal A., Swank J., 1996, ApJ 460, 470
Bessell M.S., Castelli F., Plez B., 1998, A&A 333, 231
Braun R., Strom R.G., 1986, A&AS 63, 345
Coe M.J., Pightling S.L., 1998, MNRAS 299, 223
Coe M.J., Jones L.R., Lehto H., 1994, MNRAS 270, 178
Corbet R.H.D., Smale A.P., Ozaki M., et al., 1995, ApJ 443, 786
Chakrabarty D., 1998, ApJ 492, 342
Chatterjee P., Hernquist L., Narayan R., 1999, astro-ph/9912137
Crampton D., Georgelin Y.M., Georgelin Y.P., 1978, A&A 66, 1
Cruddace R.G., Hasinger G.R., Schmitt J.H., 1988, In: Astronomy from Large Databases: Scientific objectives and methodological approaches. Proceedings of the Conference, Garching, Federal Republic of Germany, Oct. 12-14, 1987 (A89-27176 10-82), ESO conf. proceedings 28, p. 177
David L.P., Harnden F.R., Kearns K.E., et al., 1999, US ROSAT Science Data Center/SAO (http://hea–www.harvard.edu/rosat/rsdc_www/hricalrep.html)
Davies S.R., Coe M.J., 1991, MNRAS 249, 313
Fahlman G.G., Hickson P., Richer H.B., et al., 1982, ApJ 261, L1
Fesen R.A., Hurford A.P., 1995, AJ 110, 747
Fich M., Blitz L., Starke A.A., 1989, ApJ 342, 272
Gaensler B.M., Gotthelf E.V., Vasisht G., 1999, ApJ 526, L37
Ghosh P., Angelini L., White N.E., 1997, ApJ 478, 713
Gotthelf E.V., Vasisht G., 1998, NA 3, 293
Haberl F., Motch C., Buckley D.A.H., et al., 1997, A&A 326, 662
Hanson C.G., Dennerl K., Coe M.J., et al., 1988, A&A 195, 114
Hasinger G., Burg R., Giacconi R., et al., 1998, A&A 329, 482
Hellier C., 1994, MNRAS 271, L21
Hughes V.A., Harten R.H., Costain C.H., et al., 1984, ApJ 283, 147
Kahane C., Guilloteau S., Lucas R., 1985, A&A 146, 325
Kaspi V.M., Chakrabarty D., Steinberger J., 1999, ApJ 525, L33
Kouveliotou S., Dieters S., Strohmayer T., et al., 1998, Nat 393, 235
Kouveliotou S., Strohmayer T., Hurley K., et al., 1999, ApJ 510, L115
Kulkarni S.R., van Kerkwijk M.H., 1998, ApJ 507, L49
Melatos A., 1999, ApJ 519, L77
Mereghetti S., Stella L., 1995, ApJ 442, L17

Mereghetti S., Israel G.L., Stella L., 1998, MNRAS 296, 689
Monet D., Bird A., Canzian B., et al., 1998, USNO-A2.0, US Naval Observatory, Washington D.C.
Motch C., Haberl F., 1998, A&A 333, L59
Motch C., Guillot P., Haber F., et al., 1998, A&A 318, 111
Oke J.B., Cohen J.G., Carr M., et al., 1995, PASP 107, 375
Orlandini M., Dal Fiume D., Frontera F., et al., 1998, ApJ 500, L163
Paczyński B., 1990, ApJ 365, L9
van Paradijs J., McClintock J.E., 1994, A&A 290, 133
van Paradijs J., Taam R.E., van den Heuvel E.P.J., 1995, A&A 299, L41
Parmar A.N., Oosterbroek T., Favata F., et al., 1998, A&A 330, 175
Predehl P., Schmitt J.H.M.M., 1995, A&A 293, 889
Rho J., Petre R., 1997, ApJ 484, 828
Savonije G.J., de Kool M., van den Heuvel E.P.J., 1986, A&A 155, 51
Shakura N.I., Sunyaev R.A., 1973, A&A 24, 337
Sofue Y., Takahara F., Hirabayashi H., 1983, PASJ 35, 447
Stetson P.B., 1987, PASP 99, 191
Sugizaki M., Nagase F., Torii K., et al., 1997, PASJ 49, L25
Thompson C., Duncan R.C., 1996, ApJ 473, 322
Torii K., Kinugasa K., Katayama K., et al., 1998, ApJ 503, 843
Vasisht G., Gotthelf E.V., 1997, ApJ 486, L129
Vrtilek S.D., Raymond J.C., Garcia M.R., et al., 1990, A&A 235, 162
Zimmermann U., Boese G., Becker W., et al., 1998, MPE Report, ROSAT Scientific Data Center (http://wave.xray.mpe.mpg.de/exsas/users-guide)